

## Original Article

# Is stomatal conductance optimized over both time and space in plant crowns? A field test in grapevine (*Vitis vinifera*)

Thomas N. Buckley<sup>1\*</sup>, Sebastia Martorell<sup>2\*</sup>, Antonio Diaz-Espejo<sup>3</sup>, Magdalena Tomàs<sup>2</sup> & Hipólito Medrano<sup>2</sup>

<sup>1</sup>IA Watson Grains Research Centre, Faculty of Agriculture and Environment, The University of Sydney, Narrabri, NSW 2390, Australia, <sup>2</sup>Research Group on Plant Biology under Mediterranean Conditions, Departament de Biologia, Universitat de les Illes Balears, 07122 Palma de Mallorca, Spain and <sup>3</sup>Irrigation and Crop Ecophysiology Group, Instituto de Recursos Naturales y Agrobiología de Sevilla (IRNAS, CSIC), 41012 Sevilla, Spain

## ABSTRACT

**Crown carbon gain is maximized for a given total water loss if stomatal conductance ( $g_s$ ) varies such that the marginal carbon product of water ( $\partial A/\partial E$ ) remains invariant both over time and among leaves in a plant crown, provided the curvature of assimilation rate ( $A$ ) versus transpiration rate ( $E$ ) is negative. We tested this prediction across distinct crown positions *in situ* for the first time by parameterizing a biophysical model across 14 positions in four grapevine crowns (*Vitis vinifera*), computing optimal patterns of  $g_s$  and  $E$  over a day and comparing these to the observed patterns. Observed water use was higher than optimal for leaves in the crown interior, but lower than optimal in most other positions. Crown carbon gain was 18% lower under measured  $g_s$  than under optimal  $g_s$ . Positive curvature occurred in 39.6% of cases due to low boundary layer conductance ( $g_{bw}$ ), and optimal  $g_s$  was zero in 11% of cases because  $\partial A/\partial E$  was below the target value at all  $g_s$ . Some conclusions changed if we assumed infinite  $g_{bw}$ , but optimal and measured  $E$  still diverged systematically in time and space. We conclude that the theory's spatial dimension and assumption of positive curvature require further experimental testing.**

*Key-words:* boundary layer; carbon water balance; optimization; stomata; water-use efficiency.

## INTRODUCTION

Water is a major factor limiting plant growth and carbon sequestration in both natural and agricultural systems. To predict and manage these systems and to direct basic research into the underlying biological controls, we need formal mathematical models that can both predict and explain how carbon and water exchange are coordinated and regulated by stomatal conductance ( $g_s$ ). However, no

process-based model of  $g_s$  that can achieve this has yet gained consensus, and phenomenological models merely reproduce observed patterns of  $g_s$ , so they have limited ability to explain stomatal behaviour (Damour *et al.* 2010; Buckley & Mott 2013). Another approach, optimization theory, attempts to deduce  $g_s$  from the hypothesis that stomatal behaviour tends to maximize carbon gain (net CO<sub>2</sub> assimilation rate,  $A$ ) for a given water loss (transpiration rate,  $E$ ) (Cowan & Farquhar 1977). The rationale for this hypothesis is that natural selection has presumably favoured genotypes with more nearly optimal use of limiting resources, including water (Cowan & Farquhar 1977; Cowan 2002; Mäkelä *et al.* 2002).

Formally, the optimization hypothesis states that, among all possible spatiotemporal distributions of  $g_s$  that yield the same total transpiration rate, total carbon gain will be greatest for the distribution in which the ratio of the marginal sensitivities of  $A$  and  $E$  to  $g_s$  [ $(\partial A/\partial g_s)/(\partial E/\partial g_s)$ , often abbreviated as  $\partial A/\partial E$  and referred to in this study as the *marginal carbon product of water*] is invariant within the domain in which total transpiration rate can be considered constant (Cowan & Farquhar 1977). That domain is typically taken to be one day (at longer time scales, the total water supply available to the canopy, and with it the target value  $\mu$  for  $\partial A/\partial E$ , may change). This result assumes that the  $A$  versus  $E$  curve generated by varying  $g_s$  has negative curvature; that is,  $\partial A/\partial E$  always declines when  $E$  increases by stomatal opening ( $\partial^2 A/\partial E^2 < 0$ ). Pioneering work by Farquhar (1973) and Cowan & Farquhar (1977) showed that the patterns of stomatal behaviour predicted by this hypothesis share important qualitative features with the observed behaviour, including reduced  $g_s$  under high evaporative demand or low light (photosynthetic photon flux density, PPFD).

The subsequent four decades have seen this theory tested many times – most commonly in relation to controlled variations in individual environmental variables such as evaporative demand, but also in relation to natural variation in environmental conditions *in situ* (e.g. Farquhar *et al.* 1980a; Meinzer 1982; Williams 1983; Ball & Farquhar 1984; Küppers 1984; Sandford & Jarvis 1986; Guehl & Aussenac 1987; Fites

Correspondence: T. N. Buckley. Fax: +61 2 6799 2239; e-mail: t.buckley@sydney.edu.au

\*These authors contributed equally to the authorship of this work.

& Teskey 1988; Berninger *et al.* 1996; Hari *et al.* 1999; Thomas *et al.* 1999; Schymanski *et al.* 2008; Way *et al.* 2011). However, two critical elements of the original theory remain largely untested: neither its spatial dimension – that is, the prediction that  $\partial A/\partial E$  should not vary among leaves at distinct crown positions within the same individual – nor the assumption that  $\partial^2 A/\partial E^2 < 0$  have ever been tested in the field. The prediction that the target value of  $\partial A/\partial E$  should be the same for all leaves in the canopy follows from the premise that the plant has a single total water supply, and the ability, in principle, to distribute water arbitrarily among leaves. The original Cowan–Farquhar theory does not distinguish temporal and spatial variations in  $\partial A/\partial E$ , either of which will reduce whole-canopy carbon gain (provided  $\partial^2 A/\partial E^2 < 0$ ). Furthermore, few tests have accounted for variations in mesophyll and boundary layer conductances ( $g_m$  and  $g_{bc}$ , respectively), both of which restrict  $\text{CO}_2$  diffusion and can strongly influence the predictions and assumptions of optimization theory (Buckley *et al.* 1999, 2013; Buckley & Warren 2014).

The objective of this study was to test the spatial dimension of the optimization hypothesis and its assumption of negative curvature in  $A$  versus  $E$ , while accounting for mesophyll and boundary layer conductances. We parameterized a biochemical gas exchange model (which included mesophyll conductance and its temperature response) for one leaf at each of 14 standardized positions in each of the four individual crowns of grapevine (*Vitis vinifera* L. var. Grenache) and then monitored *in situ* environmental conditions and stomatal conductance for each of those leaves over time across a single day. We used these data to test the theory's assumption that  $\partial^2 A/\partial E^2 < 0$ , to infer the optimal spatiotemporal distributions of  $g_s$  (and  $E$ ) and to compare the inferred optimal patterns with the observed patterns.

## MATERIALS AND METHODS

### Study system

This study was conducted from 17 to 24 August 2012 in the experimental field of the University of Balearic Islands during summer 2012 on grapevines of Grenache varietal. Soil was a clay loam type 1.5 m deep. Plants were 3 years old grafted on rootstock Richter-110 and planted in rows (distance between rows was 2.5 m and between plants, 1 m). Plants were situated in a bilateral double cordon having between 10 and 12 canes per plant. Plants had been irrigated throughout the summer with 9.0 L per plant per day, an amount that had been established as adequate to sustain high plant water status in a previous experiment. Pre-dawn water potential of plants on the day of *in situ* gas exchange measurements (22 August 2012) was  $-0.24 \pm 0.06$  MPa.

Four plants and 14 crown positions of each plant were selected for gas exchange measurements. Four of these positions were on the east face of the crown (positions 1–4), two were on the top of the crown (positions 5 and 6), four were on the west face (positions 7–10) and four were located in the inner part of the crown (positions 11–14). These crown positions are illustrated in Fig. 1.

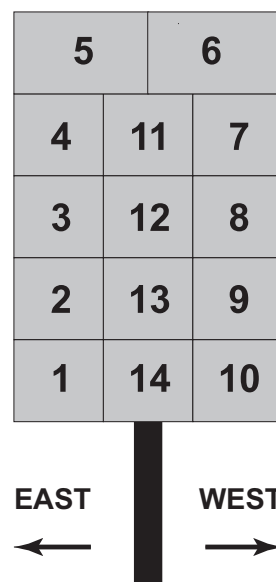


**Figure 1.** Diagram illustrating the 14 crown positions at which leaf gas exchange was measured in this study. The diagram represents a cross section of the grapevine crown, looking southward along the long axis of a planting row, with east (sunrise) to the left and west (sunset) to the right. Positions 1–10 are on the crown exterior, and positions 11–14 are in the crown interior.

### Meteorological measurements

A meteorological station (Meteodata-3000) located in the experimental field with sensors of wind speed (Young 81000, R.M. Young Company, Traverse City, MI, USA) and air temperature and relative humidity (Young 41382, Young Company) was used. The height of the wind speed sensor was 2.7 m above the soil (approximately 0.5 m above the upper part of the canopy).

### Biophysical gas exchange model

We used the photosynthesis model of Farquhar *et al.* (1980b) and the gas exchange equations of von Caemmerer & Farquhar (1981) to simulate  $\text{CO}_2$  and  $\text{H}_2\text{O}$  exchange in grapevine. Briefly, the net  $\text{CO}_2$  assimilation rate due to biochemical demand ( $A_d$ ) is computed from RuBP-carboxylation-limited and RuBP-regeneration-limited rates ( $A_v$  and  $A_j$ ) (a list of symbols is given in Table 1):

$$A_v = V_m \frac{c_c - \Gamma_*}{c_c + K_c(1 + O/K_o)} - R_d, \quad (1)$$

$$A_j = \frac{1}{4} J \frac{c_c - \Gamma_*}{c_c + 2\Gamma_*} - R_d, \quad (2)$$

where  $V_m$  is the carboxylation capacity,  $J$  is the potential electron transport rate,  $c_c$  is the chloroplastic  $\text{CO}_2$  concentration,  $\Gamma_*$  is the photorespiratory  $\text{CO}_2$  compensation point,  $K_c$  and  $K_o$  are the Michaelis constants for RuBP carboxylation and oxygenation, respectively,  $O$  is the oxygen concentration

**Table 1.** List of variables and parameters referred to in this study, including symbols, units and values where appropriate

Variable	Symbol	Units	Value
Net CO <sub>2</sub> assimilation rate	$A$	$\mu\text{mol m}^{-2} \text{s}^{-1}$	Varies
Leaf absorptance to photosynthetic photon flux	$\alpha$	–	0.92
Demand or supply limited value of $A$	$A_d, A_s$	$\mu\text{mol m}^{-2} \text{s}^{-1}$	Varies
RuBP-carboxylation or regeneration-limited value of $A_d$	$A_v, A_j$	$\mu\text{mol m}^{-2} \text{s}^{-1}$	Varies
Ambient CO <sub>2</sub> mole fraction	$c_a$	$\mu\text{mol mol}^{-1}$	400
Intercellular or chloroplastic CO <sub>2</sub> mole fraction	$c_i, c_c$	$\mu\text{mol mol}^{-1}$	Varies
Molar heat capacity of air	$c_p$	$\text{J mol}^{-1} \text{K}^{-1}$	29.2
Curvature of $A$ versus $E$ relationship	$\partial^2 A / \partial E^2$	$\mu\text{mol m}^2 \text{s mmol}^{-2}$	Varies
Saturation vapour pressure deficit of air	$D_a$	Pa	Varies
Marginal carbon product of water	$\partial A / \partial E$	$\mu\text{mol mmol}^{-1}$	Varies
Leaf characteristic dimension	$d_{\text{leaf}}$	m	0.1
Effective leaf-air water vapour mole fraction gradient	$\Delta w$	$\text{mmol mol}^{-1}$	Varies
Leaf transpiration rate	$E$	$\text{mmol m}^{-2} \text{s}^{-1}$	Varies
Leaf emissivity to IR	$\epsilon_{\text{leaf}}$	–	0.95
Fraction of absorbed photons that do not contribute to photochemistry	$f$	–	0.23
Absorbed shortwave radiation	$\Phi$	$\text{J m}^{-2} \text{s}^{-1}$	Varies
Fraction of infrared radiation that comes from the sky	$f_{\text{ir}}$	–	Varies
Psychrometric constant	$\gamma$	$\text{Pa K}^{-1}$	66.0
Photorespiratory CO <sub>2</sub> compensation point (at 25 °C)	$\Gamma^* (\Gamma_{*25})$	$\mu\text{mol mol}^{-1}$	Varies (36.2)
Leaf boundary layer conductance to heat, water or CO <sub>2</sub>	$g_{\text{bhl}}, g_{\text{bw}}, g_{\text{bc}}$	$\text{mol m}^{-2} \text{s}^{-1}$	Varies
Mesophyll conductance to CO <sub>2</sub>	$g_m$	$\text{mol m}^{-2} \text{s}^{-1}$	Varies
Radiation conductance	$g_{\text{Ra}}$	$\text{mol m}^{-2} \text{s}^{-1}$	Varies
Stomatal conductance to water or CO <sub>2</sub>	$g_s, g_{\text{sc}}$	$\text{mol m}^{-2} \text{s}^{-1}$	Varies
Maximum stomatal conductance	$g_{\text{smax}}$	$\text{mol m}^{-2} \text{s}^{-1}$	Varies
Optimal stomatal conductance	$g_{\text{so}}$	$\text{mol m}^{-2} \text{s}^{-1}$	Varies
Total leaf conductance to water or CO <sub>2</sub>	$g_{\text{tw}}, g_{\text{tc}}$	$\text{mol m}^{-2} \text{s}^{-1}$	Varies
Potential electron transport rate	$J$	$\mu\text{mol m}^{-2} \text{s}^{-1}$	Varies
Light-limited (capacity-saturated) value of $J$	$J_i$	$\mu\text{mol m}^{-2} \text{s}^{-1}$	Varies
Capacity-limited (light-saturated) value of $J$ (at 25 °C)	$J_m (J_{m25})$	$\mu\text{mol m}^{-2} \text{s}^{-1}$	Varies
Michaelis constant for RuBP carboxylation or oxygenation	$K_c, K_o$	$\mu\text{mol mol}^{-1}$	Varies
Canopy extinction coefficient for diffuse irradiance	$k_d$	–	0.8
Cumulative leaf area index	$L$	$\text{m}^2 \text{m}^{-2}$	Varies
Target value for $\partial A / \partial E$	$\mu$	$\mu\text{mol mmol}^{-1}$	1.28–1.59
Mole fraction of oxygen	$O$	$\mu\text{mol mol}^{-1}$	$2.1 \times 10^5$
Atmospheric pressure	$P_{\text{atm}}$	Pa	$1.0 \times 10^5$
Photosynthetic photon flux density	PPFD	$\mu\text{mol m}^{-2} \text{s}^{-1}$	Varies
Curvature parameter for relationship of $A_d$ to $A_v$ and $A_j$	$\theta_A$	–	0.99
Curvature parameter for relationship of $J$ to $J_m$ and $J_i$	$\theta_j$	–	0.90
Non-photorespiratory CO <sub>2</sub> release (at 25 °C)	$R_d (R_{d25})$	$\mu\text{mol m}^{-2} \text{s}^{-1}$	Varies
Net isothermal radiation	$R_n^*$	$\text{J m}^{-2} \text{s}^{-1}$	Varies
Stefan–Boltzmann constant	$\sigma$	$\text{J m}^{-2} \text{s}^{-1} \text{K}^{-4}$	$5.67 \times 10^{-8}$
Air temperature (in Kelvin)	$T_{\text{air}} (T_{\text{air,K}})$	°C (K)	Varies
Leaf temperature	$T_{\text{leaf}} (T_{\text{leaf,K}})$	°C (K)	Varies
Carboxylation capacity (at 25 °C)	$V_m (V_{m25})$	$\mu\text{mol m}^{-2} \text{s}^{-1}$	Varies
Wind speed	$v_{\text{wind}}$	$\text{m s}^{-1}$	Varies
Water vapour mole fraction of intercellular spaces or air	$w_i, w_a$	$\text{mmol mol}^{-1}$	Varies

and  $R_d$  is the rate of non-photorespiratory CO<sub>2</sub> release. Actual assimilation rate is calculated as the hyperbolic minimum of  $A_v$  and  $A_j$  [the lesser root  $A_d$  of  $\theta_A A_d^2 - A_d(A_v + A_j) + A_v A_j = 0$ , where  $\theta_A$  is a dimensionless curvature parameter less than unity]; this accounts for co-limitation by both carboxylation and regeneration near the transition between the two limitations, and it smoothes the transition, ensuring differentiability as required for continuous optimization. We calculated  $J$  as the hyperbolic minimum of light-limited and light-saturated rates,  $J_m$  and  $J_i$  [the lesser root  $J$  of  $\theta_j J^2 - J(J_m + J_i) + J_m J_i = 0$ ;  $J_i = 0.5\alpha(1 - f)\text{PPFD}$ ,  $\alpha$  is the leaf absorptance to photosynthetic

irradiance and  $f$  is the fraction of absorbed photons that do not contribute to photochemistry].

The supply of CO<sub>2</sub> by diffusion to the sites of carboxylation ( $A_s$ ) was modelled as

$$A_s = g_{\text{tc}}(c_a - c_c), \quad (3)$$

where  $g_{\text{tc}}$  is total conductance to CO<sub>2</sub>, given by

$$g_{\text{tc}} = (g_{\text{sc}}^{-1} + g_{\text{bc}}^{-1} + g_m^{-1})^{-1}, \quad (4)$$

where  $g_{\text{sc}}$  is the stomatal conductance to CO<sub>2</sub> ( $g_s/1.6$ , where  $g_s$  is the stomatal conductance to H<sub>2</sub>O),  $g_{\text{bc}}$  is the boundary layer

conductance to CO<sub>2</sub> and  $g_m$  is the mesophyll conductance to CO<sub>2</sub>. At steady state, the supply and demand rates are equal ( $A_d = A_s$ ), so the actual net CO<sub>2</sub> assimilation rate,  $A$ , is given by the intersection of  $A_d$  and  $A_s$ :

$$A = A_d \cap A_s, \quad (5)$$

This intersection leads to a quartic (fourth-order polynomial) expression for  $c_c$ , whose coefficients are functions of the parameters in Eqns 1–3, and which is readily solved for  $c_c$  (e.g. Abramowitz & Stegun 1972). Transpiration rate ( $E$ ) is given by

$$E = g_{tw} \Delta w, \quad (6)$$

where

$$g_{tw} = (g_s^{-1} + g_{bw}^{-1})^{-1}, \quad (7)$$

$$\Delta w = \frac{w_i - w_a}{1 - \frac{1}{2} \cdot 0.001 \cdot (w_i + w_a)} \quad (8)$$

in which  $g_{bw}$  is the boundary layer conductance to H<sub>2</sub>O and  $w_i$  and  $w_a$  are the water vapour mole fractions in the intercellular spaces and the ambient air, respectively. We assumed that the air spaces were saturated with water vapour, so that  $w_i$  was given by

$$w_i = 6.112 \cdot \exp[17.62 \cdot T_{leaf} / (243.13 + T_{leaf})] / P_{atm}, \quad (9)$$

where  $T_{leaf}$  is the leaf temperature in °C (World Meteorological Organization 2008). The expression in the numerator of Eqn 9 gives the saturation partial pressure of water, and  $P_{atm}$  is the total atmospheric pressure. We estimated *in situ* leaf temperature using the isothermal net radiation approximation as described by Leuning *et al.* (1995) and modified to molar units:

$$T_{leaf} = T_{air} + \frac{\gamma R_n^* / c_p - D_a g_{tw}}{s g_{tw} + \gamma (g_{bh} + g_{Rn})}, \quad (10)$$

where  $T_{air}$  is the air temperature,  $\gamma$  is the psychrometric constant,  $c_p$  is the molar heat capacity of air,  $D_a$  is the saturation vapour pressure deficit of air and  $s$  is the derivative of saturation vapour pressure with respect to temperature.  $g_{Rn}$  is the radiation conductance, given by

$$g_{Rn} = 4 \epsilon_{leaf} k_d f_{ir} \sigma T_{air}^3 / c_p, \quad (11)$$

where  $\epsilon_{leaf}$  is the leaf emissivity to longwave radiation,  $\sigma$  is the Stefan–Boltzmann constant,  $k_d$  is the canopy extinction coefficient for diffuse irradiance (0.8; Leuning *et al.* 1995) and  $f_{ir}$  is the fraction of the leaf's incoming infrared radiation that comes directly from the sky. In simulations on horizontally continuous canopies,  $f_{ir}$  is generally taken as  $\exp(-k_d L)$ , where  $L$  is the cumulative leaf area index (e.g. Leuning *et al.* 1995). We computed  $f_{ir}$  in this fashion for interior crown leaves (positions 11–14); for positions on the lateral crown exterior

(positions 1–4 and 7–10), we computed  $f_{ir}$  as the fraction of each leaf's upwards sky view occupied by actual sky rather than by the adjacent canopy [ $\beta/180$ , where  $\beta$  (degrees) is the angle at which sky appears above the adjacent canopy, as viewed from the crown position in question]. We used  $f_{ir} = 1.0$  for the two positions at the top of the crown (positions 5 and 6).  $R_n^*$  is the isothermal net radiation, given by

$$R_n^* = \Phi - (1 - \epsilon_{atm}) k_d f_{ir} \sigma T_{air,K}^4, \quad (12)$$

where  $\Phi$  is the absorbed shortwave radiation,  $\epsilon_{atm}$  is the atmospheric emissivity to longwave radiation, given by  $0.642 \cdot (0.001 \cdot P_{atm} \cdot w_a / T_{air,K})^{1/7}$  for  $P_{atm}$  in Pa and  $w_a$  in mmol mol<sup>-1</sup> (Leuning *et al.* 1995), and  $T_{air,K}$  is  $T_{air}$  in Kelvin. Note that this assumes a canopy IR emissivity of unity. We calculated  $\Phi$  by assuming that incident shortwave radiation was equal to 0.5666 · PPFD (0.5666 is the ratio of total shortwave energy to photosynthetic photon flux in extraterrestrial solar radiation; de Pury & Farquhar 1997), and that this radiation was half visible and half near-infrared (Leuning *et al.* 1995), with leaf absorptances of 0.92 and 0.2, respectively (0.92 was the mean observed PAR absorptance of leaves in this study, and 0.2 is the complement of NIR reflection and transmission coefficients, both of which are approximately 0.4; Gates *et al.* 1965). This gives  $\Phi = (0.5 \cdot 0.92 + 0.5 \cdot 0.2) \cdot 0.5666 \cdot \text{PPFD} = 0.3173 \cdot \text{PPFD}$ .

Equation 10 requires a value for boundary layer conductances to heat ( $g_{bh}$ ) and water [ $g_{bw}$ , which is embedded in  $g_{tw}$  (Eqn 7)], and Eqn 4 requires boundary layer conductance to CO<sub>2</sub> ( $g_{bc}$ ). We assumed  $g_{bc} = g_{bw}/1.37$  and  $g_{bw} = 1.08 \cdot g_{bh}$  and simulated  $g_{bh}$  using an expression based upon forced (wind-driven) convection (Leuning *et al.* 1995):

$$g_{bh} = 0.123 (v_{wind} / d_{leaf})^{0.5}, \quad (13)$$

where  $v_{wind}$  is the wind speed and  $d_{leaf}$  is the leaf's characteristic dimension (approximately equivalent to its average downwind width; 0.1 m in this study). This ignores the possibility of free convection driven by buoyancy of air warmed by the leaf. However, most available data and theoretical studies suggest that free convection contributes only negligibly to heat exchange under natural conditions, even at very low wind speeds, and that modelling  $g_{bh}$  based upon forced convection alone provides accurate predictions (Leuning 1988; Brenner & Jarvis 1995; Grantz & Vaughn 1999; Roth-Nebelsick 2001). We simulated the attenuation of wind speed through the canopy profile by

$$v_{wind} = v_{wind(top)} \cdot \exp(-0.5L), \quad (14)$$

where  $L$  is the cumulative leaf area index (m<sup>2</sup> m<sup>-2</sup>) and  $v_{wind(top)}$  is the wind speed measured above the canopy. To calculate  $L$  for each canopy position, we summed the leaf area index of all canopy regions (as defined by Fig. 1) above that position. To measure those leaf area indices, we measured the total leaf area in each canopy region for each of six individuals and then divided these areas by the projected areas of each region to give the leaf area index contributed by

that region. The resulting values of  $L$  are as follows, for positions 1–14, respectively: 3.1, 2.6, 2.1, 1.8, 0, 0, 1.5, 1.8, 2.4, 2.7, 1.6, 2.1, 2.6 and 3.3.

### Parameterizing the gas exchange model

We estimated photosynthetic parameters for each of 56 leaves (four individuals  $\times$  14 canopy positions) as follows. We measured the response of leaf net CO<sub>2</sub> assimilation rate ( $A$ ) to intercellular CO<sub>2</sub> mole fraction ( $c_i$ ) using an open flow gas exchange system (Li-6400; Li-Cor, Inc., Lincoln, NE, USA) equipped with an integrated leaf chamber fluorometer (Li-6400-40; Li-Cor). Curves were performed under saturating light ( $1500 \mu\text{mol m}^{-2} \text{s}^{-1}$ ), with block temperature controlled at 30 °C. Ambient CO<sub>2</sub> ( $c_a$ ) was set between 50 and  $1600 \mu\text{mol mol}^{-1}$  and chamber humidity was set to track ambient conditions. After steady-state photosynthesis was reached,  $c_a$  was lowered stepwise from 400 to  $50 \mu\text{mol mol}^{-1}$ , returned to  $400 \mu\text{mol mol}^{-1}$  and increased stepwise to  $1600 \mu\text{mol mol}^{-1}$ . A total of 16 points were recorded for each curve. We then estimated  $g_m$ ,  $V_m$  and  $J_m$  by the curve fitting method proposed by Ethier & Livingston (2004). To simulate changes in these parameters with temperature, we corrected these values to 25 °C (as  $g_{m25}$ ,  $V_{m25}$  and  $J_{m25}$ , respectively) using temperature responses measured on leaves of the same variety, grown in pots at the same site and transported to the laboratory to allow plants to acclimate to constant temperature and other atmospheric conditions. Temperature responses were measured by repeating CO<sub>2</sub> response curves at 15, 20, 25, 30, 35 and 40 °C, using the same protocol described above but with the expanded temperature control kit (Li-6400-88; Li-Cor) added to the gas exchange system. The temperature response data are shown in Fig. 2. Temperature response functions were as follows:

$$V_m(T_{\text{leaf,K}}) = V_{m25} \cdot \exp[a_v(T_{\text{ref}}^{-1} - T_{\text{leaf,K}}^{-1})], \quad (15)$$

$$J_m(T_{\text{leaf,K}}) = J_{m25} \cdot \exp[a_j(T_{\text{ref}}^{-1} - T_{\text{leaf,K}}^{-1})] \quad (16)$$

$$g_m(T_{\text{leaf}}) = g_{m25} \cdot \exp\left\{-d[\ln(T_{\text{leaf}}/T_{\text{opt}})]^2\right\}, \quad (17)$$

where  $T_{\text{ref}} = 298.15$  K,  $T_{\text{leaf,K}}$  is the leaf temperature in Kelvin, and  $a_v$ ,  $a_j$ ,  $b_j$ ,  $c_j$ ,  $d$  and  $T_{\text{opt}}$  are empirical parameters:  $a_v = 7350.45$  K,  $a_j = 6710.22$  K,  $b_j = -2.15188$  (unitless),  $c_j = 13\,807.8$  K,  $d = 0.71027$  (unitless) and  $T_{\text{opt}} = 36.75$  °C. Other parameters were taken from literature: 25 °C values and temperature responses for Rubisco kinetic parameters ( $K_c$  and  $K_o$ ) and the photorespiratory CO<sub>2</sub> compensation point ( $\Gamma_*$ ) were taken from Bernacchi *et al.* (2003). Non-photorespiratory CO<sub>2</sub> release in the light at 25 °C ( $R_{d25}$ ) was estimated from photosynthetic response curves as  $0.0089 \cdot V_{m25}$  according to de Pury & Farquhar (1997), and the temperature response of  $R_d$  was taken from Bernacchi *et al.* (2003).

### Measuring leaf gas exchange *in situ*

At each of five times on a given day (approximately 0915, 1100, 1345, 1600 and 1830, CEDT), we used an open flow gas

exchange system (Li-6400; Li-Cor) equipped with a clear chamber (Li-6400-08) to obtain a 30 s average measurement of stomatal conductance and incident PPFD on each of the leaves for which we had previously estimated photosynthetic parameters as described earlier. Prior to each measurement, we observed the leaf's orientation, and orientated the chamber such that the PPFD sensor surface was parallel to the original plane of the leaf; this ensured that the PPFD thus measured was very similar to the PPFD actually experienced by the leaf prior to measuring  $g_s$ ,  $c_a$  was set at  $400 \mu\text{mol mol}^{-1}$  and chamber air temperature and humidity were set to match ambient. Of the 280 expected measurements (5 times  $\times$  14 positions  $\times$  4 individuals), 10 were lost due to clerical errors, leaving 270 measurements.

### Computing $\partial A/\partial E$

We calculated  $\partial A/\partial E$  numerically, as follows. We computed  $A$  and  $E$  from the gas exchange model outlined earlier, added a very small increment ( $1.0 \times 10^{-6} \text{ mol m}^{-2} \text{ s}^{-1}$ ) to stomatal conductance and estimated  $\partial A/\partial E$  as the ratio of the resulting increases in  $A$  and  $E$ . This ensured that changes in leaf temperature ( $T_{\text{leaf}}$ ) resulting from the simulated increment in  $g_s$ , and the effects of those temperature changes on both  $A$  and  $E$ , would be calculated accurately (analytical description of the effects of changing  $T_{\text{leaf}}$  would be overly complex and prone to error, due to the many photosynthetic parameters

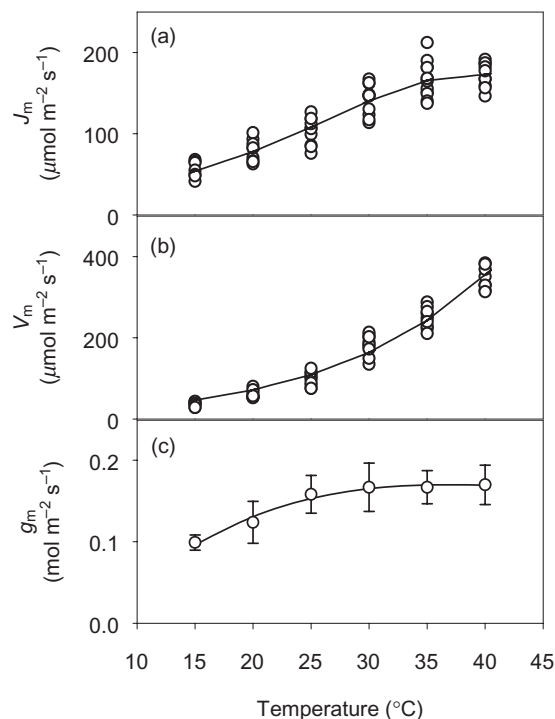


**Figure 2.** Temperature responses for photosynthetic parameters measured in grapevine for this study (symbols) and response curves fitted to these measurements (lines; Eqns 15–17 in the main text). (a) Electron transport capacity,  $J_m$ ; (b) carboxylation capacity,  $V_m$ ; and (c) mesophyll conductance to CO<sub>2</sub>,  $g_m$ .

affected by  $T_{\text{leaf}}$ ). We verified that this numerical approach did not suffer from discretization error by computing  $\partial A/\partial E$  both numerically and analytically (using expressions given by Buckley *et al.* 2002) while holding leaf temperature constant; the two resulting values of  $\partial A/\partial E$  were indistinguishable (not shown).

### Computing optimal stomatal conductance

For each point in time at each crown position, we computed optimal stomatal conductance as follows. Firstly, we generated the theoretical  $A$  versus  $E$  relationship for that point by varying  $g_s$  from  $2.0 \times 10^{-4}$  to  $2.0 \text{ mol m}^{-2} \text{ s}^{-1}$  in 10 000 steps. We then classified each point into one of three categories based upon the nature of the resulting  $A$  versus  $E$  relationship. In category I,  $\partial A/\partial E$  declines monotonically as  $g_s$  increases (i.e.  $\partial^2 A/\partial E^2 < 0$ ). In category II,  $\partial A/\partial E$  increases at low  $g_s$ , reaches a maximum and then decreases at higher  $g_s$  (i.e.  $\partial^2 A/\partial E^2 > 0$  at low  $g_s$  and  $\partial^2 A/\partial E^2 < 0$  at high  $g_s$ ). In category III,  $\partial A/\partial E$  is below its crown-wide target value ( $\mu$ , discussed below) for all positive  $g_s$  (typically because PPFD is quite low or  $\Delta w$  is quite high). Examples of relationships between  $g_s$  and  $\partial A/\partial E$  for four randomly chosen instances of each category are shown in Fig. 3a.

Identification of optimal  $g_s$  ( $g_{\text{so}}$ ) differs for each of these categories. For category III,  $g_{\text{so}}$  is zero. The category most clearly relevant to the original Cowan–Farquhar theory is category I; in this case,  $g_{\text{so}}$  is the value of  $g_s$  for which  $\partial A/\partial E$  equals a target value,  $\mu$ , that is invariant among leaves in the crown and over time (the choice of  $\mu$  is discussed below). For category II, there exists a realistic positive  $g_s$  that maximizes instantaneous water-use efficiency,  $\text{WUE} = A/E$ ; this occurs when  $A/E = \partial A/\partial E$  (Buckley *et al.* 1999) (Fig. 3b). WUE is always greater at that value of  $g_s$  than for any other value, including any value (or values) for which  $\partial A/\partial E = \mu$ . However, although this value of  $g_s$  would maximize WUE for a category II leaf considered by itself, it is not optimal for the crown as a whole. For example, imagine a category I leaf and a category II leaf both initially at  $\partial A/\partial E = \mu$  (Fig. 4a). Consider the effect of reducing  $E$  and  $g_s$  in the category II leaf in order to bring it to the point of maximum WUE, where  $\partial A/\partial E = A/E$ , and redistributing the water thus saved to the category I leaf (Fig. 4b). The total change in assimilation rate resulting from this redistribution is

$$\delta A_{\text{total}} = \int \left( \frac{\partial A}{\partial E_{\text{I}}} - \frac{\partial A}{\partial E_{\text{II}}} \right) dE, \quad (18)$$

where the subscripts I and II refer to variables in the category I and II leaves, respectively. Because  $\partial A/\partial E$  is greater in the category II leaf than in the category I leaf across the range of  $g_s$  spanning this redistribution (Fig. 4b), the integrand in Eqn 18 is negative, so the net change in assimilation rate for both leaves combined is also negative (Fig. 4c). Thus, the optimal solution when some leaves are in category II is to increase transpiration in those leaves at the expense of other leaves until  $\partial A/\partial E$  is invariant among all transpiring leaves.

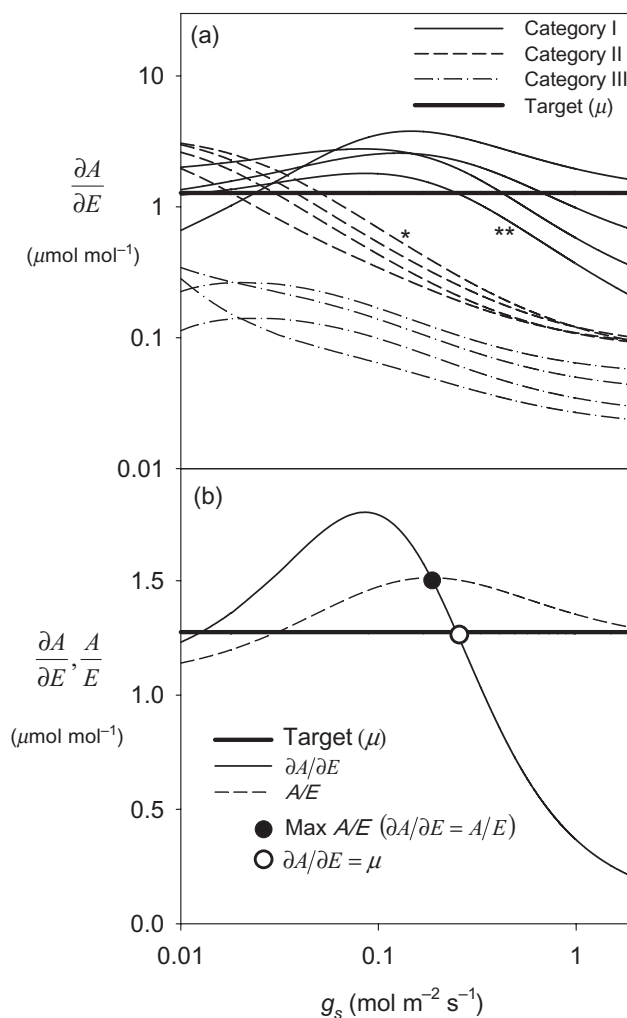


**Figure 3.** (a) Relationships between the marginal carbon product of water and  $g_s$  for four randomly chosen leaves in each of category I (for which  $\partial^2 A/\partial E^2 < 0$ ; dashed lines) and category II (for which  $\partial^2 A/\partial E^2 > 0$  at low  $g_s$ ; solid lines); the thick black horizontal line represents the target value for  $\partial A/\partial E$  ( $\mu$ ). (b) The relationships between  $g_s$  and  $\partial A/\partial E$  (solid line) and instantaneous water-use efficiency,  $A/E$  (dashed line) for one leaf in category II, showing that  $A/E$  is maximized at a lower  $g_s$  (left-hand vertical grey line) than the  $g_s$  at which  $\partial A/\partial E$  equals the crown-wide target value,  $\mu$  (right-hand vertical grey line).  $\mu$  is shown by the horizontal black line. [The curves marked with asterisks in (a) also appear in Fig. 4.]

We identified the optimal  $g_s$  in both category I and II leaves by searching the array of 10 000  $g_s$  and  $\partial A/\partial E$  values in reverse (i.e. beginning at high  $g_s$  and proceeding towards low  $g_s$ ), finding the first point where  $\partial A/\partial E > \mu$ , and identifying optimal  $g_s$  as the average of the two values spanning the change in sign of  $\partial A/\partial E$ . In 21 instances of category II points (7.8% of all points), maximum WUE occurred at  $g_s > 2.0 \text{ mol m}^{-2} \text{ s}^{-1}$ ; in these cases, we set  $g_{\text{so}}$  to  $2.0 \text{ mol m}^{-2} \text{ s}^{-1}$  on the grounds that values greater than that are not physiologically realistic. We compared the resulting distributions of water loss with alternative simulations in which  $g_{\text{so}}$  was either capped at  $1.0 \text{ mol m}^{-2} \text{ s}^{-1}$  or allowed to take on

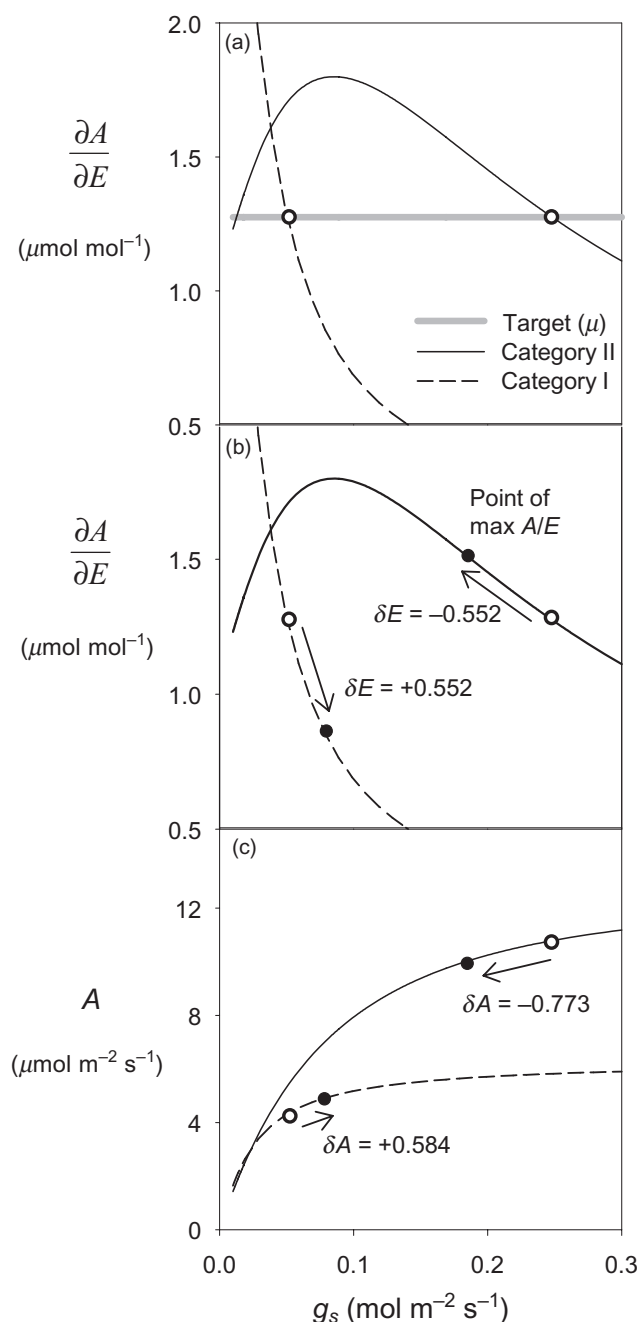


**Figure 4.** Illustration of the effect of redistributing water loss from a category II leaf (solid lines) to a category I leaf (dashed lines) in order to maximize water-use efficiency ( $A/E$ ) in the former. (a, open symbols) Initial condition, in which  $\partial A/\partial E$  equals the crown-wide target value,  $\mu$ , for both leaves. (b, closed symbols) Condition after redistribution of water loss ( $\delta E = 0.552 \text{ mmol m}^{-2} \text{ s}^{-1}$ ) from the category II leaf to the category I leaf. (c) Relationships between net  $\text{CO}_2$  assimilation rate,  $A$ , and stomatal conductance,  $g_s$ , for both leaves, with symbols representing the initial and final conditions as in (a) and (b). The net change in  $A$  resulting from redistribution is negative. (Note that the category I and II leaves correspond to the curves marked with one and two asterisks, respectively, in Fig. 3a.)

arbitrarily high values, and the results were nearly identical (not shown); this is because boundary layer conductance ( $g_{\text{bw}}$ ) was typically quite low in those instances, so that  $E$  was relatively insensitive to changes in  $g_s$ .

We identified the target value for  $\partial A/\partial E$  ( $\mu$ ) separately for each individual by adjusting an initial estimate of  $\mu$  repeatedly (re-optimizing  $g_s$  for all measurement points at each value of  $\mu$ ) until the whole-crown diurnal total water loss computed for the optimal pattern of  $g_s$  was as close as possible to the total water loss computed for the measured pattern of  $g_s$ . Because changes in  $\mu$  sometimes caused one or more measurement points to change categories, the relationship between  $\mu$  and total crown water loss was not smooth, so it was not possible to achieve arbitrarily precise agreement in crown total water use between optimal and measured  $g_s$  distributions. However, the two values agreed to within 1.53% in all cases and to within 0.21% when summed over all four crowns. To account for the effect of small remaining differences between measured and optimized crown water loss on comparisons of total carbon gain, we applied an approximate correction to total carbon gain: (Corrected optimal crown  $A$ ) = (Computed optimal crown  $A$ )  $\times$  (Measured crown  $E$ )/(Computed optimal crown  $E$ ).

## Numerical methods

All of the calculations described earlier were implemented in Microsoft Excel, in some cases using algorithms coded in VBA and in other cases using worksheet formulas. The Excel file containing the code is available from the authors upon request.

## Statistical tests of the optimization hypothesis

We chose to compare transpiration rate, rather than stomatal conductance itself, between optimal and measured patterns, for two reasons. Firstly, mean optimal  $g_s$  was many times greater than mean measured  $g_s$  in some leaves due to low boundary layer conductance (when  $g_{\text{bw}}$  is low,  $E$  is nearly insensitive to  $g_s$  at high  $g_s$ ), and this made direct comparisons between measured and optimal patterns of  $g_s$  somewhat uninformative. Secondly, because optimization theory is concerned with optimal allocation of finite resources, we felt it was more informative to compare distributions of the resource itself (water loss,  $E$ ) rather than the biological parameter ( $g_s$ ) that controls how that resource is distributed.

Residuals of  $E$  (optimal minus measured  $E$ ) were distributed highly non-normally (as were the residuals of  $g_s$ ), and normality could not be adequately improved by any transformation, so we used non-parametric tests (Kruskal–Wallis rank sum test) to assess the probability that observed systematic differences in residual  $E$  among crown positions, among times of day, and among times of day at each crown position, were due to chance alone. We also assessed variation in mesophyll conductance ( $g_{\text{m25}}$ ) with crown position using the Kruskal–Wallis test. Variations in photosynthetic capacity ( $V_{\text{m25}}$  and  $J_{\text{m25}}$ ) were distributed normally and were assessed

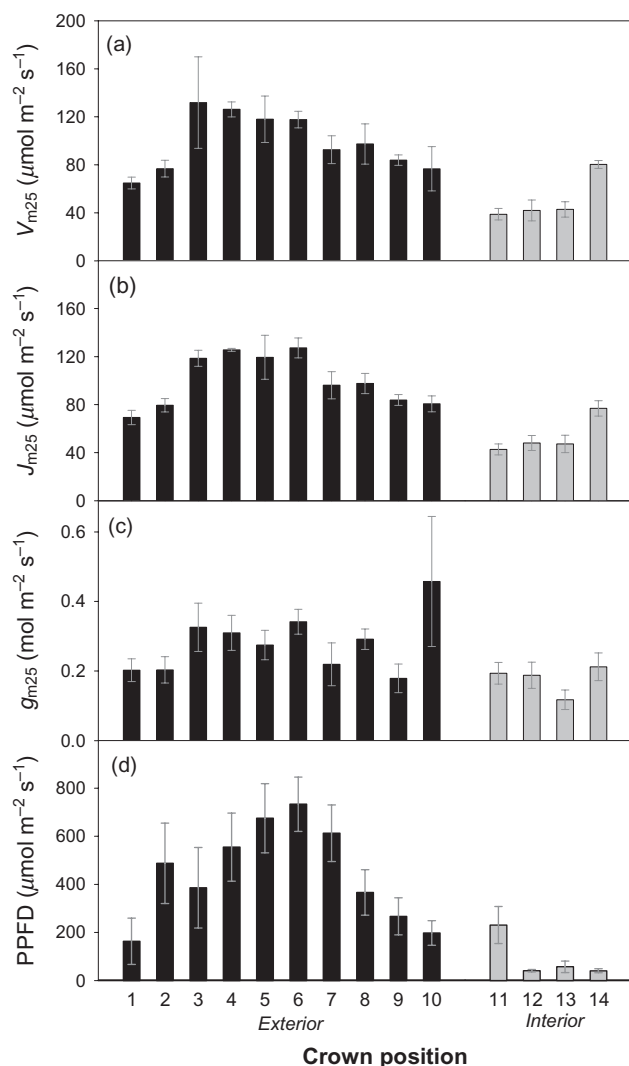


**Figure 5.** Gas exchange parameters (a, carboxylation capacity at 25 °C,  $V_{m25}$ ; b, electron transport capacity at 25 °C,  $J_{m25}$ ; c, mesophyll conductance at 25 °C,  $g_{m25}$ ) and incident photosynthetic photon flux density on the day of *in situ* measurements (d, PPFD) at each of 14 crown positions (see diagram in Fig. 1). Black bars, exterior crown; grey bars, interior crown. Sample means  $\pm$  SE.

by traditional analysis of variance in linear models. All analyses were performed in base R (Team 2013).

## RESULTS

### Photosynthetic capacity and irradiance

Photosynthetic capacity estimated from  $\text{CO}_2$  response curves ( $V_{m25}$  and  $J_{m25}$ ) differed significantly among crown positions ( $P < 0.0001$  for both variables) (Fig. 5a,b). Mesophyll conductance ( $g_{m25}$ ; Fig. 5c) also differed among positions ( $P = 0.013$ ). Each of these variables was generally greater in the upper crown (positions 4–7; Fig. 1). For comparison, mean PPFD measured *in situ* on the day of diurnal measurements (22 August 2012) was greatest at the top of the crown and

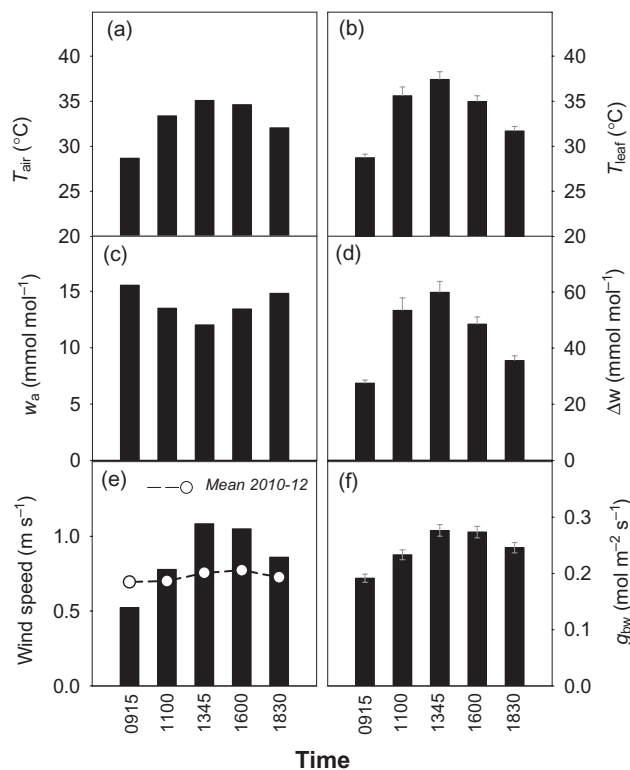


**Figure 6.** Environmental conditions measured at a meteorological station adjacent to the study site (a,c,e), and crown averages of associated leaf-level variables calculated from energy balance, based upon those environmental conditions (b, d, f). (a) Air temperature ( $T_{\text{air}}$ ); (b) leaf temperature ( $T_{\text{leaf}}$ ); (c) ambient water vapour mole fraction ( $w_a$ ); (d) effective leaf-to-air water vapour mole fraction gradient ( $\Delta w$ ); (e) wind speed ( $v_{\text{wind}}$ ) measured on the day of the study (bars) and averaged over June–August in 2010–2012 (line and symbols); (f) boundary layer conductance to water ( $g_{\text{bw}}$ ). For (b), (d) and (e), error bars are SEs among four individual crowns.

decreased down the sides of the crown, and PPFD was very low at the three lower interior crown positions (12–14) (Fig. 5d).

### Atmospheric conditions and associated leaf variables

Atmospheric conditions on 22 August 2012 were warm, calm and dry: air temperature ranged from 28.7 to 35.1 °C, ambient humidity ranged from 12.0 to 15.5  $\text{mmol mol}^{-1}$  (16.5–25.4% relative humidity) and 1 h mean wind speed ranged from 0.5 to 1.1  $\text{m s}^{-1}$  (Fig. 6). Based upon energy balance calculations, crown average leaf temperature (Fig. 6b) ranged from 28.7 to 37.4 °C, evaporative demand ( $\Delta w$ ; Fig. 6d) ranged from 27.5 to 59.9  $\text{mmol mol}^{-1}$  and boundary layer conductance ( $g_{\text{bw}}$ ; Fig. 6f) ranged from 0.19 to 0.28  $\text{mol m}^{-2} \text{s}^{-1}$ , and each of these variables peaked in early afternoon (1345 h). Stomatal conductance and water use were moderate despite these conditions, with crown average  $g_s$  ranging from a minimum of 0.06  $\text{mol m}^{-2} \text{s}^{-1}$  (at



1830 h) to a maximum of 0.13 (at 1100 h), and transpiration rate reaching a maximum of  $4.4 \text{ mmol m}^{-2} \text{ s}^{-1}$  (at 1345 h) (Fig. 7).

### Categorization of $A$ versus $E$ curves for each point

For each of 270 *in situ* measurement points, we calculated theoretical instantaneous relationships between  $A$  and  $E$  as described in the Materials and Methods section. Of these 270 points, 49.3% (133/270) were in category I, for which  $\partial A/\partial E$  declines monotonically with increasing  $g_s$ . Due to the combination of high irradiance and evaporative demand and low boundary layer conductance, we observed positive curvature in the  $A$  versus  $E$  relationship ( $\partial^2 A/\partial E^2 > 0$ ) in 39.6% (107/270) of  $A$  versus  $E$  curves. These points fall into category II, in which  $\partial A/\partial E$  increases at low  $g_s$  and decreases at high  $g_s$ . Another 11.1% (30/270) were in category III (optimal  $g_s$  was zero because  $\partial A/\partial E$  was below the target value,  $\mu$ , for all positive  $g_s$ ).

### Optimal versus observed gas exchange patterns

The optimal values of  $g_s$  were generally quite high, yet this had a smaller effect on total conductance ( $g_{\text{tw}}$ ) and hence transpiration rate ( $E$ ) than one might expect, due to the low

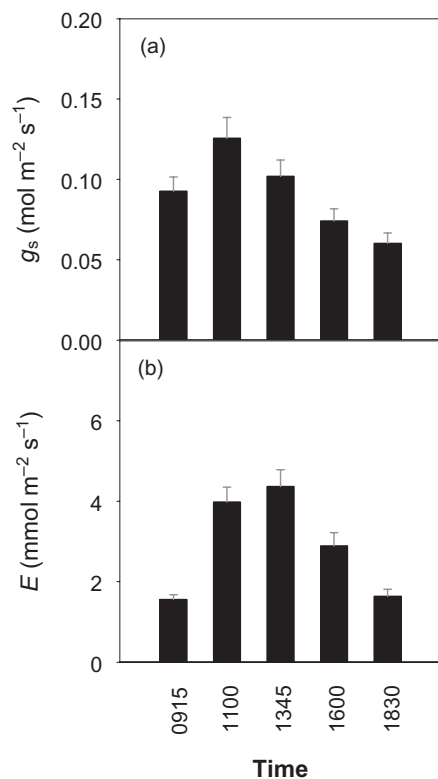


**Figure 7.** *In situ* measurements of stomatal conductance,  $g_s$  (a) and values of transpiration rate,  $E$  (b) calculated from measured  $g_s$ , averaged over 14 crown positions. Error bars are SEs among four individual crowns.

boundary layer conductances. As a consequence, mean  $g_s$  predicted by optimization greatly overestimated measured  $g_s$  in many cases, even though total crown water use was identical between the optimal and observed patterns of  $g_s$ . This is shown in panels A, C and E of Fig. 8, which present measured and predicted  $g_s$  in three ways: without any grouping (Fig. 8a), grouped by position and averaged over time (Fig. 8c), or grouped by time and averaged among positions (Fig. 8e).

Because the low boundary layer conductances led to such skewed differences between observed and optimal  $g_s$ , comparisons between observed and optimal transpiration rate ( $E$ ) are more informative and are presented in panels B, D and F of Fig. 8. Optimal  $E$  was generally greater than measured  $E$  in cases where measured  $E$  itself was higher than the crown average (Fig. 8b,d). This pattern largely reflected a re-allocation of water loss from the interior crown (positions 11–14) to the upper and east-facing exterior crown (positions 1–6), as illustrated in Fig. 9a. Residuals of  $E$  (optimal minus measured  $E$ ) differed significantly among positions ( $P < 0.0001$ ). Optimal  $E$  was also lower than measured  $E$  in the morning and higher in the late afternoon (Fig. 10a) ( $P < 0.05$ ). Additionally, the variation over time in residuals of  $E$  differed among crown positions (Fig. 11) (these changes were significant for positions 1, 2, 4, 6, 8 and 10;  $P < 0.05$ ). The clearest pattern in this regard was for optimal  $E$  to be greater than measured  $E$  in the first half of the day on the eastern crown and in the second half of the day on the western crown (Fig. 11a,c). Thus, the spatial pattern of differences between optimal and measured  $E$  among exterior crown positions shown in Fig. 9 partly reflects a time-by-position interaction.

### Effects of gas exchange distributions on total carbon gain

To assess how whole plant carbon/water balance would be impacted by these differences between measured and optimal patterns of water use, we computed total diurnal carbon gain for each crown in three ways: using either the measured or optimal spatiotemporal distributions of  $g_s$  or using a constant value of  $g_s$ , while controlling for total crown water loss in each case. We found that a constant  $g_s$  yielded  $71.7 \pm 0.6\%$  of the total carbon gain achieved by the optimal  $g_s$  distribution, whereas the observed  $g_s$  distribution achieved  $81.8 \pm 0.3\%$  of the optimum (Fig. 12).

### Effects of aerodynamic coupling (boundary layer conductance)

Because boundary layer conductance impacts the validity of the assumption that  $\partial^2 A/\partial E^2 < 0$ , which underlies optimization theory, we repeated all calculations under an alternative scenario in which  $g_{\text{bw}}$  was imagined to be extremely large (which we simulated by setting wind speed to  $3 \times 10^8 \text{ m s}^{-1}$ ). The purpose of comparing the original results to this alternative scenario was to assess the sensitivity of inferred optima to assumptions about aerodynamic coupling between leaves and the air. Some conclusions were qualitatively

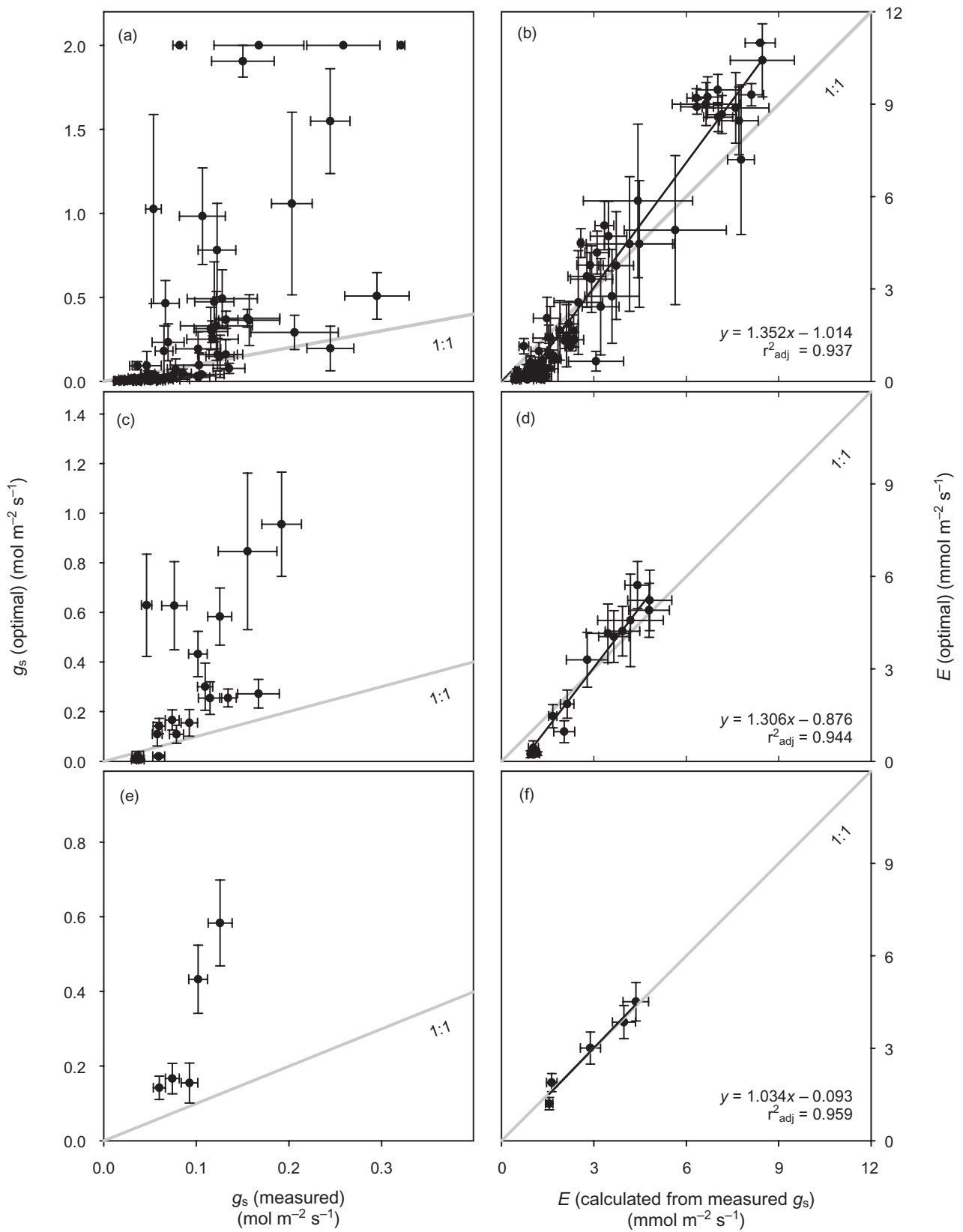


**Figure 8.** Measured versus optimal stomatal conductance to H<sub>2</sub>O  $g_s$  (a, c, e) and transpiration rate,  $E$  (b, d, f). (a, b) Averages within each of 70 combinations of crown position and measurement time. (c, d) Averages over all measurement times within each of 14 crown positions. (e, f) Averages over all crown positions at each of five measurement times. Error bars are SEs among four individual crowns. Grey lines in (b), (d) and (f): one-to-one line. Note the y-axis scales differ in (a), (c) and (e).

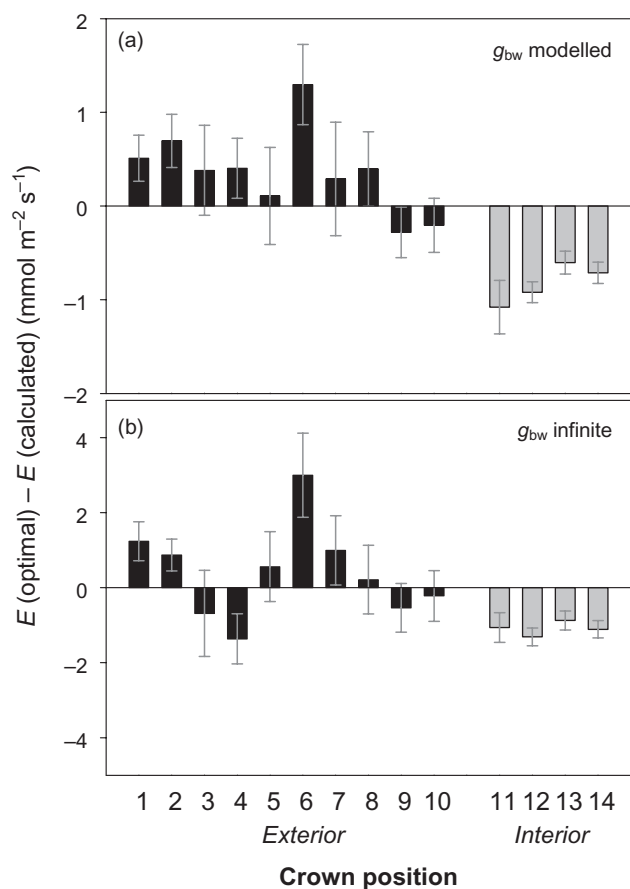


**Figure 9.** Residuals of transpiration rate (optimal minus measured  $E$ ): diurnal means in relation to crown position. (a) Optimal  $E$  computed using boundary layer conductance,  $g_{bw}$ , modelled based upon measured wind speed. (b) Optimal  $E$  computed assuming negligible boundary layer resistance (infinite  $g_{bw}$ ). Error bars are SEs among four individual crowns. Note the y-axis scales differ in (a) and (b).

similar between the 'decoupled' and 'coupled' scenarios: for example, in both scenarios, the optimal pattern shifted water use from the interior crown to the upper exterior crown (cf. Fig. 9a,b), and from early in the day to later in the day. However, some conclusions differed as well. For example, the optimal pattern shifted water use away from positions 3 and 4 on the east face (cf. Fig. 9a,b). The magnitude of redistribution of water loss required to achieve the optimum was also greater at many positions in the coupled scenario than in the decoupled scenario (e.g. position 6; cf. Fig. 9a,b), although the difference in total carbon gain between the observed  $g_s$  distribution and the theoretical optimum was smaller in the coupled scenario (11.6% versus 18.2%) (Fig. 12)

## DISCUSSION

Our objective was to test two aspects of stomatal optimization theory that have largely been ignored by previous studies. Most work has focused upon the prediction that stomata should keep the marginal carbon product of water,

$\partial A/\partial E$ , invariant over time. However, the theory also predicts that stomata must hold  $\partial A/\partial E$  invariant in space (i.e. among leaves in distinct environments within the same individual crown) and it assumes that water loss earns diminishing returns in terms of carbon gain (i.e. the curvature of  $A$  versus  $E$  is negative:  $\partial^2 A/\partial E^2 < 0$ ) (Cowan & Farquhar 1977), yet these aspects of the theory remain largely untested. Our results suggest that neither the spatial aspect of the theory nor its assumption of negative curvature hold in grapevine canopies under the hot, dry, sunny and calm conditions typical of Mediterranean summer at our study site. We found that the measured spatial pattern of water use differed systematically from the optimal pattern, with some regions of the crown using more water than the optimum and other regions using less. We also found positive curvature in  $A$  versus  $E$  for 40% of leaf measurements, largely due to low boundary layer conductance. In addition, we found that if we had simply assumed negligible boundary layer resistance, as many applications of the theory have assumed, then the resulting predictions would have diverged substantially from the true optima, thereby altering some conclusions about the relationship between observed and optimal patterns.

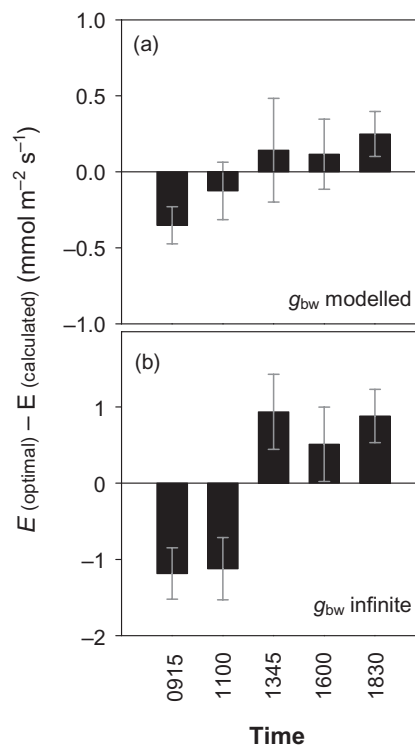


**Figure 10.** Residuals of transpiration rate (optimal minus measured  $E$ ): averages over 14 crown positions, shown in relation to time. (a) Optimal  $E$  computed using boundary layer conductance,  $g_{bw}$ , modelled based upon measured wind speed. (b) Optimal  $E$  computed assuming negligible boundary layer resistance (infinite  $g_{bw}$ ). Error bars are SEs among four individual crowns. Note the y-axis scales differ in (a) and (b).

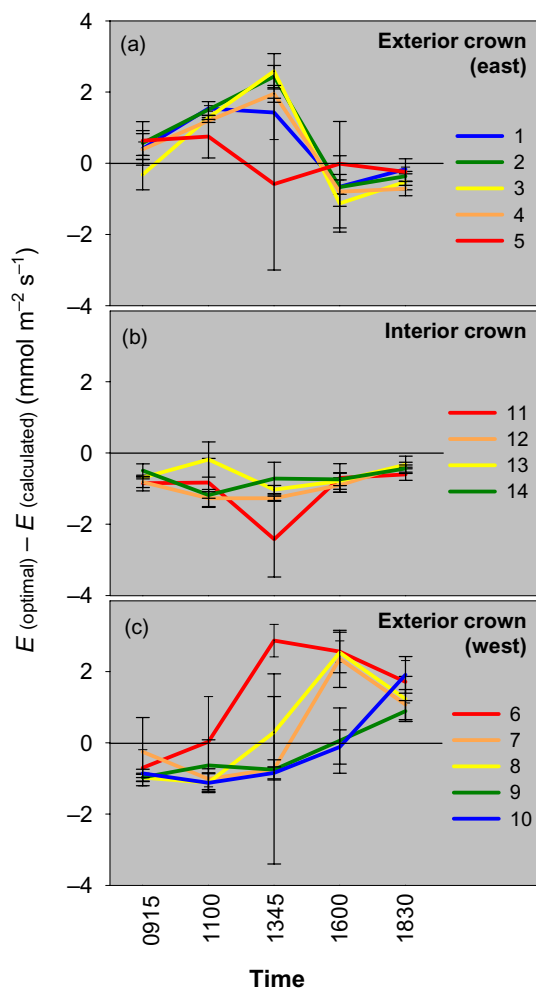


**Figure 11.** Residuals of transpiration rate (optimal minus measured  $E$ ) over time for each of 14 crown positions: (a) positions 1–5 (the eastern side of the crown); (b) positions 11–14 (the interior crown); (c) positions 6–10 (the western side of the crown). Error bars are SEs among four individual crowns.

### Positive curvature in $A$ versus $E$ and its implications

Water loss typically brings diminishing returns of carbon gain because stomatal opening tends to reduce the gradient for leaf  $\text{CO}_2$  uptake more than that for  $\text{H}_2\text{O}$  loss. As  $g_s$  increases, intercellular  $\text{CO}_2$  increases, this decreases the  $\text{CO}_2$  gradient. Although a related effect occurs with transpiration – that is, increased  $E$  can decrease the evaporative gradient ( $\Delta w$ ) by increasing ambient humidity – this effect is generally smaller than the  $\text{CO}_2$  effect because the volume of air even in a dense canopy is vastly larger than the volume of the intercellular air spaces (Cowan 1977; Buckley *et al.* 1999). In this case, there is no instantaneous optimum for the trade-off between carbon gain and water loss: carbon gain per unit of water loss (instantaneous water-use efficiency,  $\text{WUE} = A/E$ ) is greatest in the limit of zero  $g_s$ , which is a trivial solution. This is what led Cowan & Farquhar (1977) to ask what pattern of  $g_s$  maximizes total carbon gain for a given total

water loss, which leads to the invariant- $\partial A/\partial E$  solution. However, increased  $g_s$  can strongly reduce  $\Delta w$  when boundary layer conductance ( $g_{bw}$ ) is low. This is because low  $g_{bw}$  weakens convective heat transfer, increasing the scope of evaporative cooling to reduce leaf temperature and therefore  $\Delta w$  (Jones 1992). The resulting changes in  $\Delta w$  can lead to positive curvature in  $A$  versus  $E$  (Cowan 1977; Buckley *et al.* 1999). In such conditions, there is an instantaneous optimum for leaf-scale WUE, which occurs when  $\partial A/\partial E = A/E$  (the point at which the tangent line to the  $A$  versus  $E$  curve goes through the origin) (Buckley *et al.* 1999). As a result, it is initially unclear whether the invariant- $\partial A/\partial E$  solution still applies in such conditions.

Buckley *et al.* (1999) suggested that if curvature is positive but a leaf cannot maintain  $E$  high enough to reach the maximum  $A/E$ , then the leaf should close some stomata entirely and open others more widely to achieve the optimum in the latter areas; that is, spatially heterogeneous  $g_s$  is beneficial in this case. A related argument can be made at the crown level. If some leaves have negative curvature and others have positive curvature, then water loss should be re-allocated from the former to the latter to allow the latter to maximize WUE. This will reduce  $E$  in the negative curvature leaves, thereby increasing  $\partial A/\partial E$  and WUE in those leaves as well and ensuring that the re-allocation improves WUE throughout the crown. Furthermore, whole-crown WUE is maximized by increasing  $g_s$  even further in leaves with positive curvature – that is, beyond the point at which WUE is maximized for those individual leaves – as explained in the text surrounding Eqn 18 and illustrated in Fig. 4.

The Cowan & Farquhar (1977) solution therefore applies even if positive curvature occurs, provided curvature eventu-

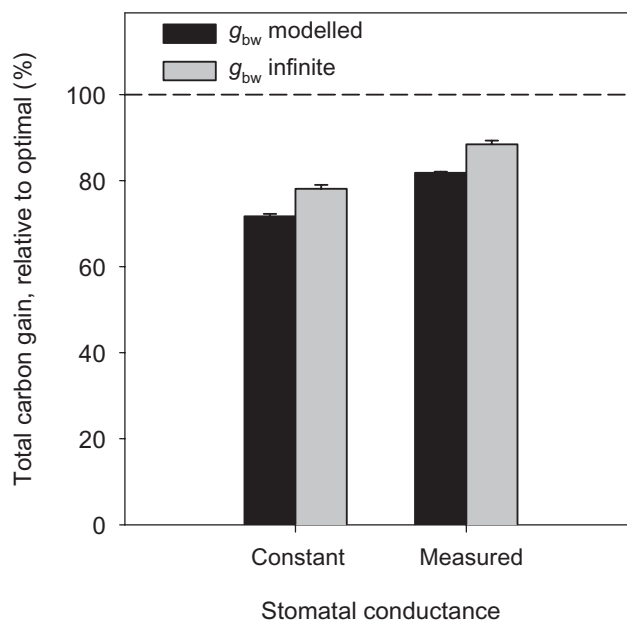


**Figure 12.** Total diurnal carbon gain calculated using either constant  $g_s$ , measured  $g_s$  or optimized  $g_s$ , expressed as a percentage of optimized values. Error bars are SEs among four individual crowns.

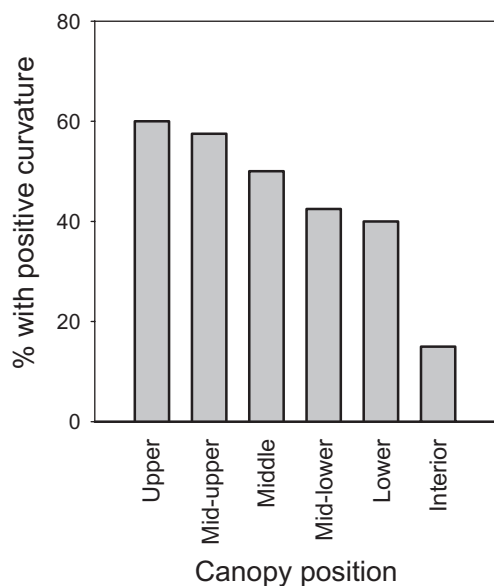


**Figure 13.** Proportion (as percent) of measurement points for which positive curvature in the relationship between assimilation rate and transpiration rate was observed. Position categories are as follows: upper (positions 5 and 6), mid-upper (positions 4 and 7), middle (positions 3 and 8), mid-lower (positions 2 and 9), lower (positions 1 and 10) and interior (positions 11–14). Position numbers are shown in Fig. 1.

ally becomes negative at higher  $g_s$ . There are two exceptions to this solution. Firstly, stomata should simply open as far as possible in leaves in which  $\partial A/\partial E$  is always greater than the crown-wide target value ( $\mu$ ). This scenario applied in 7.8% of measured leaves in the present study. In these cases, boundary layer conductance was very low, so that changes in  $g_s$  had very little effect on  $\partial A/\partial E$  at high  $g_s$ . Secondly, stomata should simply close in leaves for which the crown-wide target value of  $\partial A/\partial E$  ( $\mu$ ) cannot be reached for any  $g_s$  ('category III' leaves in our terminology; Fig. 3a); this scenario applied in 11.1% of leaves in this study.

The implications of positive curvature will depend upon how often, in nature, boundary layer conductance is low enough to allow positive curvature to occur. Wind speed above the canopy ranged from 0.5 to 1.1  $\text{m s}^{-1}$  in our study, and positive curvature occurred across this range. This range is low but not particularly unusual for our site: mean daytime summer wind speed was 0.69–0.77  $\text{m s}^{-1}$  over 2010–2012 (Fig. 6e). Another study on grapevine (Daudet *et al.* 1998) found wind speed was below 1.0  $\text{m s}^{-1}$  for 13% of a typical day, and Jones *et al.* (2002) found wind speed rarely exceeded 1.3  $\text{m s}^{-1}$  during 2 of 4 days in a field study on grapevine. Similar ranges have been reported in other species (e.g. 1–2  $\text{m s}^{-1}$ , cotton; Grantz & Vaughn 1999). Wind speed is much lower inside the crown because of wind attenuation by the canopy itself (e.g. Oliver 1971, Daudet *et al.* 1999, Grantz & Vaughn 1999). However, this was not a dominant factor in causing positive curvature in the present study, as the occurrence of positive curvature actually decreased with depth in the canopy (Fig. 13). We conclude that the occurrence of

positive curvature in  $A$  versus  $E$  may not be as rare as previously thought, and that the matter requires further experimental study.

### Why is the spatial distribution of water loss suboptimal?

We found that the observed distribution of water loss among leaves did not match the optimal pattern, that the residuals were systematically related to crown position and that these deviations reduced crown carbon gain by 18% compared to the optimum. It is helpful here to reiterate the rationale for this definition of 'optimal': total carbon gain will be greatest for a given total water loss if  $\partial A/\partial E$  is invariant (provided  $\partial^2 A/\partial E^2 > 0$ ). That statement is independent of spatial or temporal scale and is a generic mathematical result from the calculus of variations (Cowan & Farquhar 1977). It says that among all possible spatiotemporal distributions of  $g_s$  that give the same total crown water loss, carbon gain is greatest for the distribution in which  $\partial A/\partial E$  is invariant. A separate question is, at what scale is it biologically meaningful to view total water loss as invariant (Cowan 1982, 1986; Mäkelä *et al.* 1996; Buckley & Schymanski 2014)? In the next section ('Is the optimization problem correctly posed?'), we discuss the possibility that it is not biologically appropriate to view total crown water loss as invariant, regardless of time scale. In this section, we discuss other possible explanations for the observed spatial deviations from optimality. One involves delays in stomatal opening. We found that optimal water loss typically exceeded observed water loss whenever the sun was orientated most directly towards a particular crown position (e.g. Fig. 11). It is possible that stomata in these positions could not respond quickly enough to the peak in PPFD to achieve optimal water loss. This effect would be exacerbated by low  $g_{bw}$ , which requires large changes in  $g_s$  to achieve a given change in water loss. Vico *et al.* (2011) suggested that delays in stomatal opening and closing in response to changes in PPFD create a quasi-optimal pattern of  $g_s$ , arguing that the costs of stomatal regulation itself must be subtracted from leaf net carbon gain in computing the optimum, so that the true optimum includes a finite time constant for stomatal adjustments to PPFD. This is unlikely to explain our results, given that the carbon cost of stomatal movements was on the order of 0.25% of net assimilation rate in the simulations presented by Vico *et al.* (2011) – far less than the potential improvement in carbon gain that could have been achieved by optimal stomatal control in our study.

Medlyn *et al.* (2011, 2013) suggested that stomata lack the physiological machinery to detect the shift between carboxylation- and regeneration-limited photosynthesis. Those authors noted that stomatal responses to short-term changes in atmospheric  $\text{CO}_2$  were approximately optimal under regeneration-limited but not carboxylation-limited conditions, so they suggested that stomata were only capable of optimal behaviour under regeneration-limited conditions (i.e. under sub-saturating PPFD). Our results offer qualified support for that idea, as deviations from optimality at a given position tended to be greater when the sun was orientated

more directly towards that position, at which time PPFD would likely be saturating.

The spatial distribution of photosynthetic nitrogen may also have contributed to these deviations. The ratio of carboxylation capacity to PPFD was eight times greater in the interior crown (positions 11–14) than on the upper exterior crown (positions 4–7) (Fig. 5) – consistent with other reports that capacity is not proportional to local irradiance, contrary to the predictions of optimization theory for distribution of photosynthetic nitrogen (Evans 1993; Hirose & Werger 1994; Hollinger 1996; Makino *et al.* 1997; de Pury & Farquhar 1997; Bond *et al.* 1999; Friend 2001; Frak *et al.* 2002; Kull 2002; Lloyd *et al.* 2010; Buckley *et al.* 2013). It is well established that  $g_s$  is highly correlated with photosynthetic capacity (Wong *et al.* 1979). If this correlation represents a mechanistic constraint on stomatal regulation – that is, if the mechanisms that stomata have presumably evolved to optimize carbon/water balance include a physiological ‘response’ to photosynthetic capacity or some proxy thereof – then, such a response may present a physiological barrier to achieving optimal distributions of water loss in situations where photosynthetic capacity is suboptimally distributed. This highlights the important linkage between the economics of water loss and photosynthetic nitrogen use in plant crowns (Field 1983; Buckley *et al.* 2002, 2013; Farquhar *et al.* 2002; Peltoniemi *et al.* 2012; Buckley & Warren 2014; Palmroth *et al.* 2013).

### Is the optimization problem correctly posed?

The requirement that  $\partial A/\partial E$  be spatially invariant within the crown assumes that water loss can be arbitrarily allocated among leaves and over time within the crown. However, hydraulic constraints may make it impossible for leaves in some crown positions to achieve optimal water loss rates while also maintaining water potential above thresholds for catastrophic loss of hydraulic conductivity. Although this could be remedied by increasing hydraulic conductance to such leaves by re-allocating carbon, such re-allocation may itself be suboptimal, for two reasons. One is that stem carbon serves other functions, including mechanical support. Another is that hydraulic limitations to water loss may only manifest during brief periods in the growing season, in which case the large carbon investment needed to achieve optimal distribution of water loss may outweigh any resulting gains in crown WUE. Thus, each leaf may, in fact, require a different target value for  $\partial A/\partial E$  to reflect the realities of its water supply constraints. A full exploration of this idea requires more intensive theoretical analysis.

### Conclusions

We found systematic divergence between observed and optimal spatial patterns of water use, and evidence of widespread positive curvature ( $\partial^2 A/\partial E^2 > 0$ ) in grapevine crowns under hot, dry and calm conditions. Positive curvature resulted from aerodynamic decoupling between the crown and atmosphere. Our results suggest that caution is war-

ranted when using optimization theory to predict  $g_s$  at the crown scale, and that further study is required to assess the occurrence of conditions leading to positive curvature. We also suggest that it may be necessary to revise optimization theory to account for variations in hydraulic capacity within a crown.

### ACKNOWLEDGMENTS

This work was funded by the Spanish Ministry of Science and Innovation (research projects AGL2008-04525-C02-01, AGL2011-30408-C04-01 and AGL2009-11310/AGR). T.N.B. was supported by the US National Science Foundation (Award No. 1146514) and by the Grains Research and Development Corporation (GRDC). S.M. benefitted from a FPI grant BES-2009-016906 from the Spanish Ministry of Science and Innovation. The authors thank Dr Joan Cuxart for the meteorological data, Stan Schymanski and Graham Farquhar for helpful conversations, and two anonymous reviewers and the Associate Editor, Dr Danielle Way, for helpful comments on an earlier draft. We are particularly indebted to a reviewer who noted a critical error in our identification of optimal  $g_s$  in category II leaves.

### REFERENCES

- Abramowitz M. & Stegun I.A. (1972) Solutions of quartic equations. In *Handbook of Mathematical Functions with Formulas, Graphs and Mathematical Tables*, pp. 17–18. Dover, New York.
- Ball M.C. & Farquhar G.D. (1984) Photosynthetic and stomatal responses of two mangrove species, *Aegiceras corniculatum* and *Avicennia marina*, to long term salinity and humidity conditions. *Plant Physiology* **74**, 1–6.
- Bernacchi C., Pimentel C. & Long S. (2003) *In vivo* temperature response functions of parameters required to model RuBP-limited photosynthesis. *Plant, Cell & Environment* **26**, 1419–1430.
- Berninger F., Mäkelä A. & Hari P. (1996) Optimal control of gas exchange during drought: empirical evidence. *Annals of Botany* **77**, 469–476.
- Bond B.J., Farnsworth B.T., Coulombe R.A. & Winner W.E. (1999) Foliage physiology and biochemistry in response to light gradients in conifers with varying shade tolerance. *Oecologia* **120**, 183–192.
- Brenner A.J. & Jarvis P.G. (1995) A heated leaf replica technique for determination of leaf boundary layer conductance in the field. *Agricultural and Forest Meteorology* **72**, 261–275.
- Buckley T.N. & Mott K.A. (2013) Modelling stomatal conductance in response to environmental factors. *Plant, Cell & Environment* **36**, 1691–1699.
- Buckley T.N. & Schymanski S.J. (2014) Stomatal optimisation in relation to atmospheric CO<sub>2</sub>. *New Phytologist* **201**, 372–377.
- Buckley T.N. & Warren C.R. (2014) The role of mesophyll conductance in the economics of nitrogen and water use in photosynthesis. *Photosynthesis Research* **119**, 77–88.
- Buckley T.N., Farquhar G.D. & Mott K.A. (1999) Carbon-water balance and patchy stomatal conductance. *Oecologia* **118**, 132–143.
- Buckley T.N., Miller J.M. & Farquhar G.D. (2002) The mathematics of linked optimisation for nitrogen and water use in a canopy. *Silva Fennica* **36**, 639–669.
- Buckley T.N., Cescatti A. & Farquhar G.D. (2013) What does optimisation theory actually predict about crown profiles of photosynthetic capacity, when models incorporate greater realism? *Plant, Cell & Environment* **36**, 1547–1563.
- von Caemmerer S. & Farquhar G.D. (1981) Some relationships between the biochemistry of photosynthesis and the gas exchange of leaves. *Planta* **153**, 376–387.
- Cowan I. (2002) Fit, fitter, fittest; where does optimisation fit in? *Silva Fennica* **36**, 745–754.
- Cowan I.R. (1977) Stomatal behaviour and environment. *Advances in Botanical Research* **4**, 117–228.

- Cowan I.R. (1982) Water use and optimization of carbon assimilation. In *Encyclopedia of Plant Physiology. 12B. Physiological Plant Ecology* (eds O.L. Lange, C.B. Nobel, C.B. Osmond & H. Ziegler), pp. 589–630. Springer-Verlag, Berlin.
- Cowan I.R. (1986) Economics of carbon fixation in higher plants. In *On the Economy of Plant Form and Function* (ed. T.J. Givnish), pp. 133–170. Cambridge University Press, Cambridge.
- Cowan I.R. & Farquhar G.D. (1977) Stomatal function in relation to leaf metabolism and environment. *Symposium of the Society for Experimental Biology* **31**, 471–505.
- Damour G., Simonneau T., Cocharid H. & Urban L. (2010) An overview of models of stomatal conductance at the leaf level. *Plant, Cell & Environment* **33**, 1419–1438.
- Daudet F., Silvestre J., Ferreira M., Valancogne C. & Pradelle F. (1998) Leaf boundary layer conductance in a vineyard in Portugal. *Agricultural and Forest Meteorology* **89**, 255–267.
- Daudet F., Le Roux X., Sinoquet H. & Adam B. (1999) Wind speed and leaf boundary layer conductance variation within tree crown: consequences on leaf-to-atmosphere coupling and tree functions. *Agricultural and Forest Meteorology* **97**, 171–185.
- Ethier G. & Livingston N. (2004) On the need to incorporate sensitivity to CO<sub>2</sub> transfer conductance into the Farquhar–von Caemmerer–Berry leaf photosynthesis model. *Plant, Cell & Environment* **27**, 137–153.
- Evans J.R. (1993) Photosynthetic acclimation and nitrogen partitioning within a lucerne canopy. II. Stability through time and comparison with a theoretical optimum. *Australian Journal of Plant Physiology* **20**, 69–82.
- Farquhar G.D. (1973) *A Study of the Responses of Stomata to Perturbations of Environment*. The Australian National University, Canberra, Australia.
- Farquhar G.D., Schulze E.D. & Kupperts M. (1980a) Responses to humidity by stomata of *Nicotiana glauca* L. and *Corylus avellana* L. are consistent with the optimization of carbon dioxide uptake with respect to water loss. *Australian Journal of Plant Physiology* **7**, 315–327.
- Farquhar G.D., von Caemmerer S. & Berry J.A. (1980b) A biochemical model of photosynthetic CO<sub>2</sub> assimilation in leaves of C<sub>3</sub> species. *Planta* **149**, 78–90.
- Farquhar G.D., Buckley T.N. & Miller J.M. (2002) Stomatal control in relation to leaf area and nitrogen content. *Silva Fennica* **36**, 625–637.
- Field C.B. (1983) Allocating nitrogen for the maximization of carbon gain: leaf age as a control on the allocation program. *Oecologia* **56**, 341–347.
- Fites J. & Teskey R. (1988) CO<sub>2</sub> and water vapor exchange of *Pinus taeda* in relation to stomatal behavior: test of an optimization hypothesis. *Canadian Journal of Forest Research* **18**, 150–157.
- Frak E., Le Roux X., Millard P., Adam B., Dreyer E., Escuit C., ... Varlet-Grancher C. (2002) Spatial distribution of leaf nitrogen and photosynthetic capacity within the foliage of individual trees: disentangling the effects of local light quality, leaf irradiance, and transpiration. *Journal of Experimental Botany* **53**, 2207–2216.
- Friend A.D. (2001) Modelling canopy CO<sub>2</sub> fluxes: are ‘big-leaf’ simplifications justified? *Global Ecology and Biogeography* **10**, 603–619.
- Gates D.M., Keegan H.J., Schleter J.C. & Weidner V.R. (1965) Spectral properties of plants. *Applied Optics* **4**, 11–20.
- Grantz D.A. & Vaughn D.L. (1999) Vertical profiles of boundary layer conductance and wind speed in a cotton canopy measured with heated brass surrogate leaves. *Agricultural and Forest Meteorology* **97**, 187–197.
- Guehl J.-M. & Aussenac G. (1987) Photosynthesis decrease and stomatal control of gas exchange in *Abies alba* Mill. in response to vapor pressure difference. *Plant Physiology* **83**, 316–322.
- Hari P., Mäkelä A., Berninger F. & Pohja T. (1999) Field evidence for the optimality hypothesis of gas exchange in plants. *Australian Journal of Plant Physiology* **26**, 239–244.
- Hirose T. & Werger M.J.A. (1994) Photosynthetic capacity and nitrogen partitioning among species in the canopy of a herbaceous plant community. *Oecologia* **100**, 203–212.
- Hollinger D.Y. (1996) Optimality and nitrogen allocation in a tree canopy. *Tree Physiology* **16**, 627–634.
- Jones H.G. (1992) *Plants and Microclimate*, 2nd edn. Cambridge University Press, Cambridge.
- Jones H.G., Stoll M., Santos T., de Sousa C., Chaves M.M. & Grant O.M. (2002) Use of infrared thermography for monitoring stomatal closure in the field: application to grapevine. *Journal of Experimental Botany* **53**, 2249–2260.
- Kull O. (2002) Acclimation of photosynthesis in canopies: models and limitations. *Oecologia* **133**, 267–279.
- Küppers M. (1984) Carbon relations and competition between woody species in a central European hedgerow. II. Stomatal responses, water use, and hydraulic conductivity in the root/leaf pathway. *Oecologia* **64**, 344–354.
- Leuning R. (1988) Leaf temperatures during radiation frost. Part II. A steady state theory. *Agricultural and Forest Meteorology* **42**, 135–155.
- Leuning R., Kelliher F.M., de Pury D.G.G. & Schulze E.D. (1995) Leaf nitrogen, photosynthesis, conductance and transpiration: scaling from leaves to canopies. *Plant, Cell and Environment* **18**, 1183–1200.
- Lloyd J., Patino S., Paiva R.O., Nadrdo G.B., Quesada C.A., Santos A.J.B., ... Mercado L.M. (2010) Optimisation of photosynthetic carbon gain and within-canopy gradients of associated foliar traits for Amazon forest trees. *Biogeosciences* **7**, 1833–1859.
- Makino A., Sato T., Nakano H. & Mae T. (1997) Leaf photosynthesis, plant growth and nitrogen allocation in rice under difference irradiances. *Planta* **203**, 390–398.
- Mäkelä A., Berninger F. & Hari P. (1996) Optimal control of gas exchange during drought: theoretical analysis. *Annals of Botany* **77**, 461–467.
- Mäkelä A., Givnish T.J., Berninger F., Buckley T.N., Farquhar G.D. & Hari P. (2002) Challenges and opportunities of the optimality approach in plant ecology. *Silva Fennica* **36**, 605–614.
- Medlyn B.E., Duursma R.A., De Kauwe M.G. & Prentice I.C. (2013) The optimal stomatal response to atmospheric CO<sub>2</sub> concentration: Alternative solutions, alternative interpretations. *Agricultural and Forest Meteorology*.
- Medlyn B.E., Duursma R.A., Eamus D., Ellsworth D.S., Prentice I.C., Barton C.V.M., Crous K.Y., De Angelis P., Freeman M. & Wingate L. (2011) Reconciling the optimal and empirical approaches to modelling stomatal conductance. *Global Change Biology*, **17**, 2134–2144.
- Meinzer F. (1982) The effect of vapor pressure on stomatal control of gas exchange in Douglas fir (*Pseudotsuga menziesii*) saplings. *Oecologia* **54**, 236–242.
- Oliver H. (1971) Wind profiles in and above a forest canopy. *Quarterly Journal of the Royal Meteorological Society* **97**, 548–553.
- Palmroth S., Katul G.G., Maier C.A., Ward E., Manzoni S. & Vico G. (2013) On the complementary relationship between marginal nitrogen and water-use efficiencies among *Pinus taeda* leaves grown under ambient and CO<sub>2</sub>-enriched environments. *Annals of Botany* **111**, 467–477.
- Peltoniemi M.S., Duursma R.A. & Medlyn B.E. (2012) Co-optimal distribution of leaf nitrogen and hydraulic conductance in plant canopies. *Tree Physiology* **32**, 510–519.
- de Pury D.G.G. & Farquhar G.D. (1997) Simple scaling of photosynthesis from leaves to canopies without the errors of big-leaf models. *Plant, Cell & Environment* **20**, 537–557.
- Roth-Nebelsick A. (2001) Computer-based analysis of steady-state and transient heat transfer of small-sized leaves by free and mixed convection. *Plant, Cell & Environment* **24**, 631–640.
- Sandford A.P. & Jarvis P.G. (1986) Stomatal responses to humidity in selected conifers. *Tree Physiology* **2**, 89–103.
- Schymanski S.J., Roderick M.L., Sivapalan M., Hutley L.B. & Beringer J. (2008) A canopy-scale test of the optimal water-use hypothesis. *Plant, Cell & Environment* **31**, 97–111.
- Team R.C. (2013) *R: A Language and Environment for Statistical Computing*. R Foundation for Statistical Computing, Vienna, Austria.
- Thomas D.S., Eamus D. & Bell D. (1999) Optimization theory of stomatal behaviour: II. Stomatal responses of several tree species of north Australia to changes in light, soil and atmospheric water content and temperature. *Journal of Experimental Botany* **50**, 393–400.
- Vico G., Manzoni S., Palmroth S. & Katul G. (2011) Effects of stomatal delays on the economics of leaf gas exchange under intermittent light regimes. *The New Phytologist* **192**, 640–652.
- Way D.A., Oren R., Kim H.-S. & Katul G.G. (2011) How well do stomatal conductance models perform on closing plant carbon budgets? A test using seedlings grown under current and elevated air temperatures. *Journal of Geophysical Research: Biogeosciences* **116**, G04031.
- Williams W.E. (1983) Optimal water-use efficiency in a California shrub. *Plant, Cell & Environment* **6**, 145–151.
- Wong S.C., Cowan I.R. & Farquhar G.D. (1979) Stomatal conductance correlates with photosynthetic capacity. *Nature* **282**, 424–426.
- World Meteorological Organization (2008) *Guide to Meteorological Instruments and Methods of Observation*. WMO, Geneva, Switzerland.

Received 15 December 2013; received in revised form 21 March 2014; accepted for publication 24 March 2014